Environ Sci Pollut Res (2013) 20:3639–3648
DOI 10.1007/s11356-012-1272-7

RESEARCH ARTICLE

Simultaneous adsorption and degradation of Zn^{2+} and Cu^{2+} from wastewaters using nanoscale zero-valent iron impregnated with clays

Li-Na Shi · Yan Zhou · Zuliang Chen · Mallavarapu Megharaj · Ravi Naidu

Received: 29 August 2012 / Accepted: 19 October 2012 / Published online: 1 November 2012

Abstract Clays such as kaolin, bentonite and zeolite were evaluated as support material for nanoscale zero-valent iron (nZVI) to simultaneously remove Cu^{2+} and Zn^{2+} from aqueous solution. Of the three supported nZVIs, bentonite-supported nZVI (B-nZVI) was most effective in the simultaneous removal of Cu^{2+} and Zn^{2+} from a aqueous solution containing a 100 mg/l of Cu^{2+} and Zn^{2+}, where 92.9 % Cu^{2+} and 58.3 % Zn^{2+} were removed. Scanning electronic microscope (SEM) revealed that the aggregation of nZVI decreased as the proportion of bentonite increased due to the good dispersion of nZVI, while energy dispersive spectroscopy (EDS) demonstrated the deposition of copper and zinc on B-nZVI after B-nZVI reacted with Cu^{2+} and Zn^{2+}. A kinetics study indicated that removing Cu^{2+} and Zn^{2+} with B-nZVI accorded with the pseudo first-order model. These suggest that simultaneous adsorption of $Cu^{2+}$and Zn^{2+} on bentonite and the degradation of $Cu^{2+}$and Zn^{2+} by nZVI on the bentonite. However, Cu^{2+} removal by B-nZVI was reduced rather than adsorption, while Zn^{2+} removal was main adsorption. Finally, Cu^{2+}, Zn^{2+}, Ni^{2+}, Pb^{2+} and total Cr from various wastewaters were removed by B-nZVI, and reusability of B-nZVI with different treatment was tested, which demonstrates that B-nZVI is a potential material for the removal of heavy metals from wastewaters.

Keywords Clays · Nanoscale zero-valent iron · Wastewater · Reuse

Responsible editor: Vinod Kumar Gupta

L.-N. Shi · Y. Zhou · Z. Chen (✉)
School of Environmental Science and Engineering,
Fujian Normal University,
Fuzhou 350007, Fujian, China
e-mail: zlchen@fjnu.edu.cn

Z. Chen · M. Megharaj · R. Naidu
Centre for Environmental Risk Assessment and Remediation,
University of South Australia,
Mawson Lakes, SA 5095, Australia

Z. Chen · M. Megharaj · R. Naidu
Cooperative Research Centre for Contamination
Assessment and Remediation of Environments,
Mawson Lakes, SA 5095, Australia

Introduction

Remediation of heavy metals has attracted attention owing to the fact that they entail severe risks for the environment and human health (Järup 2003; Gupta et al. 2009, 2012a; Jain et al. 2004). The United States Environmental Protection Agency (USEPA) proposed a report on priority pollutants, listing 129 kinds of severe hazard contaminants, including copper and zinc (Keith and Telliard 1979; Gupta and Sharma 2003). Various conventional techniques have been developed for the treatment of heavy metals in wastewaters, such as chemical precipitation (Lin et al. 2005), oxidation–reduction (Chen et al. 2008; Gupta et al. 2007a,b), ion exchange (Keane 1998), adsorption (Bhattacharyya and Gupta 2008; Gupta et al. 2010, 2011a; Gupta and Nayak 2011; Gupta et al. 2006, 2012a; Saleh and Gupta 2012), biosorption (Sarioglu et al. 2009; Gupta et al. 2009; Gupta and Rastogi 2009 Gupta et al. 2012b, c), and electrochemical methods (Feng et al. 2007; Gupta et al. 2007c). However, some of these techniques have limitations due to their low efficiency and high operational cost. An alternative method known as nanoremediation, which entails using various nanomaterials to transform and detoxify pollutants, has received attention during the last decade (Nowack and Bucheli 2007; Saleh and Gupta 2011; Gupta et al. 2011b). Of these, nanoscale zero-valent iron (nZVI) is the most widely used for in situ remediation due to its large surface area, rapid reactivity and better injectability into aquifers. nZVI has been proved to be effective in the remediation of various pollutants in aqueous

solution, including chlorinated hydrocarbon, chlorinated benzenes, nitrocompounds and heavy metals (Zhang 2003; Li et al. 2006).

Challenges remain in the real application of nZVI, including the aggregation of nZVI particles, which has resulted from a large surface area being present and ultimately leads to a decrease in the reactivity of nZVI. To address this issue, strategies have been developed such as impregnation of the nanoparticles on the surface of support materials (Shahwan et al. 2010; Shi et al. 2011). The removal of $Cr_2O_7^{-2}$ and Pb^{2+} by polymeric resin-supported nZVI has been reported (Ponder et al. 2000). More recently, the removal of Pb^{2+} using kaolin supported nZVI has been reported (Zhang et al. 2011), where a concept of the simultaneous adsorption of Pb^{2+} on kaolin and the degradation of Pb^{2+} by nZVI on the kaolin supported nZVI has been proposed. Despite clay such as kaolin can be used to remove heavy metals from aqueous solution (Jiang et al. 2010). However, the adsorbed contaminants could be released in to the environment and pose potential risks to ecosystems. The simultaneous adsorption and degradation of Pb^{2+} occurring on the kaolin supported nZVI materials suggest that this is a promising method for remediation of metals ions. In addition, heavy metals in electroplating wastewater contain various heavy metals as co-contaminants. A few studies have been published on simultaneous removal of heavy metals by supported nZVI. Hence, removal behaviours of heavy metals and the relevant mechanism may help to understand simultaneous removal of heavy metals, where the mechanism is still unclear.

Mineral clays are low-cost, abundant and stable, and therefore kaolin and bentonite were used as support material for nZVI to remove metals $Cr_2O_7^{-2}$ and Pb^{2+} and (Shi et al. 2011; Zhang et al. 2011) in our previous reports, but there is no report on clay as the support nZVI to examine these support materials affecting the removal of metals. In this report, mineral clays such as kaolin, bentonite and zeolite were evaluated as support materials for nZVI and used to simultaneously remove heavy metals such as Cu^{2+} and Zn^{2+}. Hence, the aims of this study were: (1) synthesis of the support materials of nZVI; (2) characterization of the materials with scanning electronic microscopy (SEM), EDX and BET-N_2 techniques; (3) kinetics of Cu^{2+} and Zn^{2+} removal by B-nZVI; and (4) demonstrating firstly the removal of heavy metals from wastewater using B-nZVI, and secondly the reusability of B-nZVI.

Materials and methods

Materials and chemicals

Bentonite and kaolin used in this study are natural low-grade minerals without any modification, and were supplied by Longyan Kaolin Co. Ltd. (Fujian, China). These materials were ground and sieved through a 200-mesh after being dried at 80 °C overnight. The zeolite was chemically pure with a granular size of 200 mesh. All other regents used in this study were analytically pure and distilled water was used in all preparations. A highly concentrated stock solution of Cu^{2+} and Zn^{2+} was prepared by dissolving $Cu(NO_3)_2$ or $Zn(NO_3)_2$ with distilled water simultaneously or separately and stored under 5 °C.

Synthesis of nZVI and supported nZVI

The nZVI and supported nZVIs were prepared using conventional liquid-phase methods by reducing ferric iron with borohydride, which necessitated mineral clay acting as a support material (Shahwan et al. 2010; Zhang et al. 2011). Support material (2.00 g) was initially placed into a three-necked open flask, and a ferric solution produced by dissolving ferric chloride hexa-hydrate (9.66 g) in an ethanol/water solution (50 ml, 4:1 v/v) was added and stirred for 10 min. Subsequently, a freshly prepared $NaBH_4$ solution (3.54 g of $NaBH_4$ in 100 ml) was added dropwise into the mixture and constant stirred for 20 min. The whole process described above was performed under a N_2 atmosphere with vigorous stirring so that the B-nZVI did not oxidize. The synthetic reaction occurred as below (Shi et al. 2011)

$$4Fe^{3+} + BH_4^- + 3H_2O \rightarrow 4Fe^{2+} + H_2BO_3^- + 4H^+ + 2H_2 \uparrow \quad (1)$$

$$2Fe^{2+} + BH_4^- + 3H_2O \rightarrow 2Fe^0 \downarrow + H_2BO_3^- + 4H^+ + 2H_2 \uparrow \quad (2)$$

$$4Fe^{3+} + 3BH_4^- + 9H_2O \rightarrow 4Fe^0 \downarrow + 3H_2BO_3^- + 12H^+ + 6H_2 \uparrow \quad (3)$$

The formed suspension was filtered and the black nanoscale precipitate was washed three times with pure ethanol and dried overnight at 75 °C under vacuum (Shahwan et al. 2010). The theoretical mass fraction of mineral clay in synthesized B-nZVI was 50 %, and nZVI was prepared under identical conditions but with mineral clay omitted. The supported nZVI was labeled as B-nZVI, K-nZVI or Z-nZVI, when the support material was bentonite, kaolin or zeolite, respectively. nZVI and supported nZVI samples were stored in brown, sealed bottles in a dry environment and were not acidified prior to use. In subsequent experiments, unsupported nZVI and B-nZVI with different mass ratios of bentonite versus nZVI, which were theoretically calculated to be 0:1, 1:1, 2:1, 3:1 and 4:1, were prepared by

varying the initial bentonite loadings at the beginning of the synthesis.

Characterizations and measurements

SEM images and energy dispersive spectroscope (EDS) patterns of various materials were obtained with a Philips-FEI XL30 ESEM-TMP (Philips Electronics Co., Eindhoven, the Netherlands) instrument.

The specific surface areas (SSA) of nZVI, B-nZVI and bentonite were measured using the BET-N_2 method using Micromeritics' ASAP 2020 Accelerated Surface Area and Porosimetry Analyzer (Micromeritics Instrument Corp., Georgia, USA).

Batch experiments

In order to select the support material, B-nZVI, K-nZVI and Z-nZVI (ratio of support material/nZVI was 1:1) were used to remove Cu^{2+} and Zn^{2+}, respectively. Next, 0.075 g supported-nZVI was added into 25-ml mixed solutions with the initial concentrations of both Cu^{2+} and Zn^{2+} at 100 mg/l without pH adjustment.

To determine the optimal mass ratios of bentonite/nZVI in B-nZVI, which were set at 0:1, 1:1, 2:1, 3:1 and 4:1 in the synthesis procedure, B-nZVI with different mass ratios were tested for their efficiency in removing Cu^{2+} and Zn^{2+} with the initial concentration at 100 mg/l. The theoretic dosage of iron was fixed at 1 g/l. In addition, bentonite was applied to remove Cu^{2+} and Zn^{2+} independently to examine the role that bentonite played in the B-nZVI.

Batch experiments were conducted to investigate the kinetics of Cu^{2+} and Zn^{2+} removal via B-nZVI (2:1). The effects of different initial concentrations of Cu^{2+} and Zn^{2+} ions and temperatures were tested, which were set at 20, 50, 70, 100 mg/l and 20 °C, 25 °C, 30 °C, and 35 °C, respectively. Each batch experiment was mixed with 25 ml Cu^{2+} and Zn^{2+} solution. The initial concentrations of both ions were set at 100 mg/l in the rotary shaker at 35 °C and 250 rpm, and then filtered through 0.45-μm MCE membranes prior to establishing the concentrations of Cu^{2+} and Zn^{2+} at selected timed intervals.

To investigate the capacity of B-nZVI (2:1) for the removal of heavy metal ions from wastewater, two electroplating wastewaters and one dyeing wastewater were collected from the manufacturer (Fuzhou, China). The wastewater was centrifuged at 3,000 rpm for 10 min to remove all solid impurities prior to determining the initial pH and initial concentrations of various heavy metal ions. Next, 25 ml wastewater was added to the batch of centrifugal tubes containing 0.10 g of B-nZVI (2:1), which were kept on a rotary shaker at 35 °C and 250 rpm for 2 h. Then, the pH and concentration of each heavy metal ion were determined.

Reuse experiments were done to evaluate the reusability of B-nZVI for removing Cu^{2+} and Zn^{2+} from mixed solution. B-nZVI (2:1) (0.1 g) was mixed with 20 or 50 mg/l Cu^{2+} and Zn^{2+} solution (25 ml), respectively, for 1 h (35 °C and 250 rpm) before being centrifuged at 3,000 rpm. All supernates were transferred carefully into clean containers to determine the residual concentrations of Cu^{2+} and Zn^{2+} while the used B-nZVI left in the bottom was mixed with another 25 ml Cu^{2+} and Zn^{2+} solution directly or after being treated. The used B-nZVI was treated by mixing with 25 ml distilled water and then 2 % HNO_3 for 15 min, respectively. Each series of reuse was successively carried out three times.

The concentrations of Cu^{2+}, Zn^{2+} and other heavy metal ions were found using a flame atomic absorbance spectrometer (Varian AA 240FS, USA). In order to ensure the accuracy and reliability of the data, batch experiments were carried out at least in triplicate.

Results and discussion

Synthesis of various clays-supported nZVI

Cu^{2+} and Zn^{2+} removal using clays-supported nZVI

Studies have been shown where different clays such as kaolin (Zhang et al. 2009) and bentonite (Shi et al. 2011) were used to support nZVI, but no report has described the effect on the impregnation of nZVI using various clays. Hence, bentonite, kaolin and zeolite were used to support nZVI in this study. The initial pH value of Cu^{2+} and Zn^{2+} mixed solution was around 3.9 without adjustment. Figure 1 shows that the removal capacity of Cu^{2+} and Zn^{2+} using such various supported nZVIs are in order of decreasing effectiveness: bentonite support nZVI (B-nZVI)>kaolin support nZVI (K-nZVI)>zeolite support nZVI (Z-nZVI). It can be seen that B-nZVI was the most efficient material for removing both Cu^{2+} and Zn^{2+}. The removal of 92.9 % Cu^{2+} and 58.3 % Zn^{2+} was observed after 3 h using B-nZVI, while only 48.1 % Cu^{2+} and 7.6 % Zn^{2+} were removed by Z-nZVI. However, the removal of Cu^{2+} using various support materials of nZVI was much more efficient than that of Zn^{2+}.

The poor removal of Cu^{2+} and Zn^{2+} using Z-nZVI resulted from the poor dispersion of nZVI on the surface of zeolites due to the porous material of zeolite having three-dimensional structures (Mohan and Pittman 2006). In addition, the zeolite used in this study with a micrometer-scaled diameter made the dispersion of the nZVI particles on zeolite ineffective. In this case, most nZVI particles existed without being supported. Kaolin and bentonite used in this study were natural minerals, where bentonite had a major component of montmorillonite >90 %. Compared to the 1:1 layer structure of kaolin, montmorillonite had a three-layer

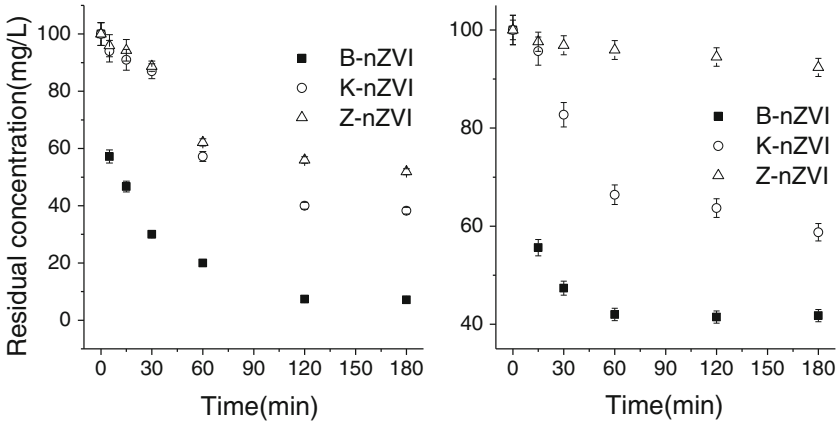

Fig. 1 The removal of Cu^{2+} and Zn^{2+} by supported nZVI with different support materials. **a** Cu^{2+} ion; **b** Zn^{2+} ion

structure composed of silica–alumina–silica units, leading to an easier cleavage and expansion between the layers in aqueous solution. The net layer charges of kaolin and montmorillonite are 0 and −0.8 charge/unit cell, respectively (Bhattacharyya and Gupta 2008). This resulted in an interaction between the core–shell structure of nZVI and the shell composed of iron oxide and hydroxide, since the surface of the nZVI particles had positive net charges (Li and Zhang 2006, 2007). As a result, bentonite was more favorable for dispersing nZVI particles through electrostatic interactions. In addition, bentonite emerged as being more effective in improving the activity of nZVI since it has a flexible lamellar structure. It was therefore selected as the best support material for nZVI for further study.

Furthermore, a more efficient removal of Cu^{2+} than that of Zn^{2+} was observed as mentioned above. This is because the standard reduction potential of Cu^{2+} ($\Phi^0_{Cu^{2+}/Cu^0}$= 0.337 V) is more positive than that of Zn^{2+}($\Phi^\theta_{Zn^{2+}/Zn^0}$= −0.762 V), meaning that Cu^{2+} is much easier to be reduced compared with Zn^{2+} (Ladd 2004). On the other hand, the adsorption of both Cu(II) and Zn(II) onto the negatively charged bentonite surface or the nZVI surface, which may include electrostatic interactions and specific surface bonding (Bhattacharyya and Gupta 2008; Li and Zhang 2007) were possible. However, adsorption could be dominated in the removal of Zn^{2+} while reduction may play a main role in the removal of Cu^{2+}. This is also supported by the XPS spectra of nZVI after reacting with various heavy metal ions in aqueous solution (Li and Zhang 2007).

Mass ratios of bentonite/nZVI and their influence on Cu^{2+} and Zn^{2+} removal

Bentonite can be used to absorb Cu^{2+} and Zn^{2+} with a low removal capacity (Bhattacharyya and Gupta 2008). To examine the adsorption of Cu^{2+} and Zn^{2+} on the bentonite, batch experiments were conducted utilizing co-adsorption of Cu^{2+} and Zn^{2+}, and results showed that only 5.5 % of Cu^{2+} and 9.8 % Zn^{2+} adsorbed on bentonite. This indicates that bentonite can be as adsorbent to remove a small part of Cu^{2+} and Zn^{2+} — this is due to the decrease of available adsorption sites after being used as the support material for nZVI —— and the removal of Cu^{2+} and Zn^{2+} is dominated by the absorption and reduction by nZVI and bentonite using B-nZVI (Zhang 2003; Bhattacharyya and Gupta 2008).

The removal efficiencies of Cu^{2+} and Zn^{2+} using B-nZVI are shown in Fig. 2, which was prepared with different mass ratios of bentonite/nZVI (0:1, 1:1, 2:1, 3:1 and 4:1). It can be seen that the removal efficiencies of Cu^{2+} and Zn^{2+} varied according to the mass ratios of bentonite/nZVI, which increased as the mass ratio rose from 0:1 to 2:1. The highest removal efficiency of Cu^{2+} and Zn^{2+} was approximately 76.5 % and 42.3 %, respectively, using B-nZVI with mass ratios of bentonite/nZVI (2:1). This can be interpreted by the SEM images of unsupported nZVI and B-nZVI (Figs. 3 and 4). They show that the unsupported nanoparticles were severely aggregated, and the aggregation decreased as the proportion of bentonite increased.

The decrease in aggregation led to an increase in the SSA of the nanoparticles, and hence an increase in the number of

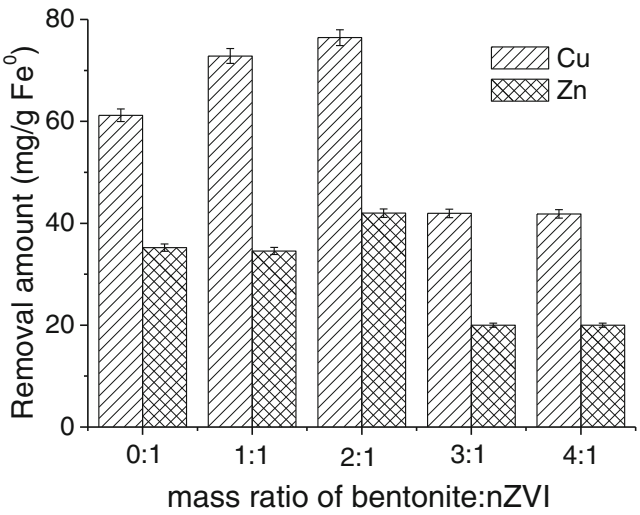

Fig. 2 Removal efficiencies of Cu^{2+} and Zn^{2+} ion using B-nZVI with different mass ratios of bentonite/nZVI

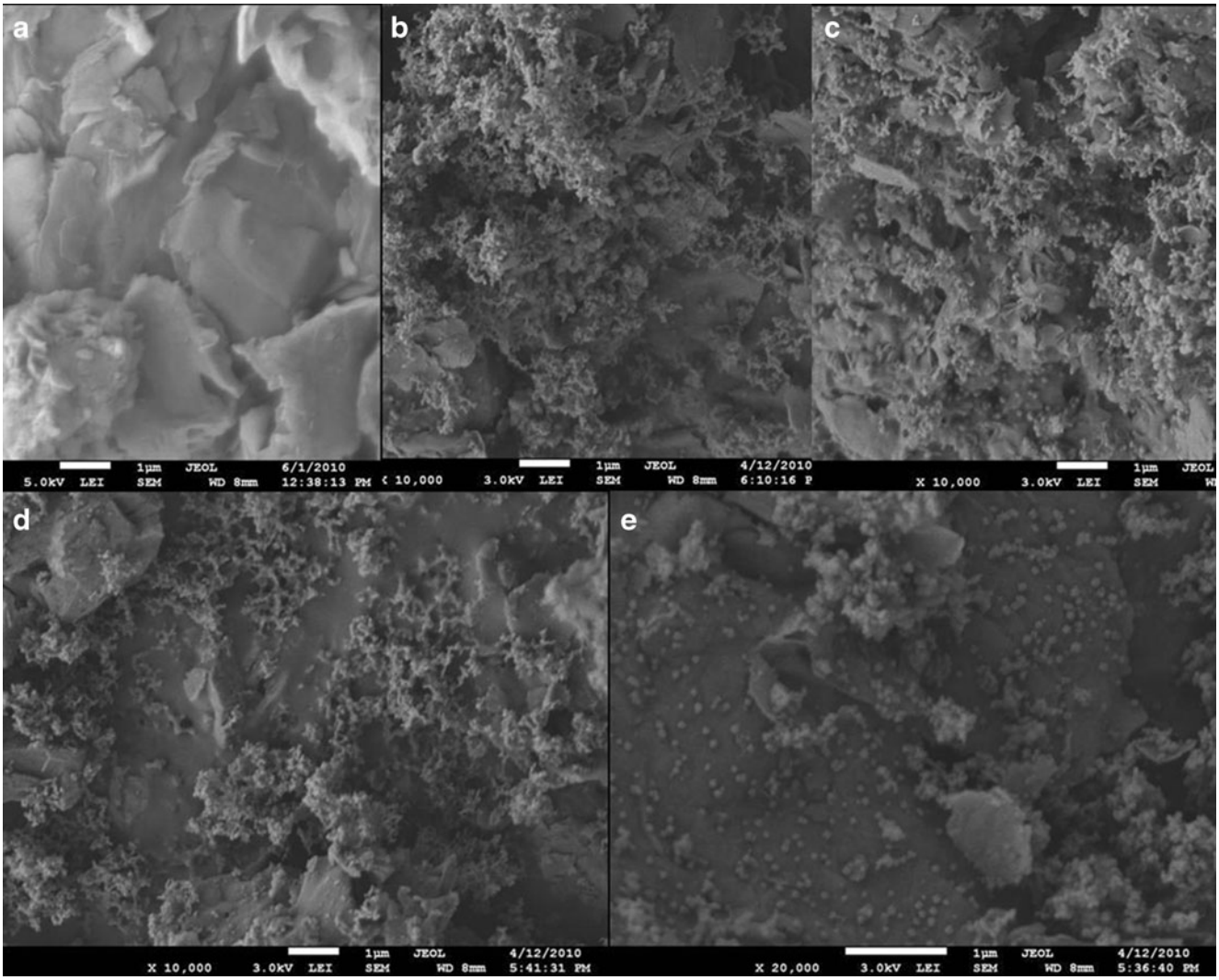

Fig. 3 SEM images of B-nZVI with different mass ratios of bentonite/nZVI. **a** Bentonite; **b** B-nZVI (1:1); **c** B-nZVI (2:1); **d** B-nZVI (3:1); **e** B-nZVI (4:1)

active sites (Zhang et al. 2011). However, the removal efficiencies were equally poor when the mass ratios rose to 3:1 and 4:1, which were approximately 50.2 % of the efficiencies by B-nZVI (2:1). This was because the high content of bentonite blocked the formation of nZVI during synthesis, and consequently resulted in a decline of the amount of iron nanoparticles dispersed on bentonites (Shahwan et al. 2010). Additionally, the higher dispersion of nZVI accelerated the oxidation and deterioration of zero-valent iron (Wang et al. 2010). Hence, B-nZVI (2:1) was used in the subsequent study.

Characterization

The SEM images of bentonite and B-nZVI are presented in Fig. 3, which showed that the nanoparticles that adhered to the surface of bentonite are generally spherical in shape and have diameters within 100 nm. However, nZVI accumulated into a bulky nanocluster, which can be attributed to their natural tendency to remain in a more thermodynamically stable state since they have a huge SSA as previously reported (Zhang et al. 2009, 2011). Figure 3 shows that the proportion of separate iron nanoparticles that scatter on the surface of bentonite seems to increase as the ratio of bentonite increases. The surface area of the bentonite support increased with increasing bentonite content, leading to decreased aggregation and improved nanoparticle dispersion (Shi et al. 2011). This occurred even when the nZVI continued to interconnect with one another and formed a chain-like morphology. Bentonite was demonstrated to be effective in reducing the aggregation and accelerating the dispersion of nanoparticles, which was consistent with the observation of kaolinite used as a support material (Shahwan et al. 2010).

The SSAs for bentonite, nZVI, and B-nZVI were 6.03, 54.04 and 26.91 m^2/g, respectively. Despite a low SSA of B-nZVI being obtained compared to that of nZVI, a high rate of removal of Cu^{2+} and Zn^{2+} was achieved using B-nZVI. Contributing to this was the decrease in nZVI aggregation and a subsequent

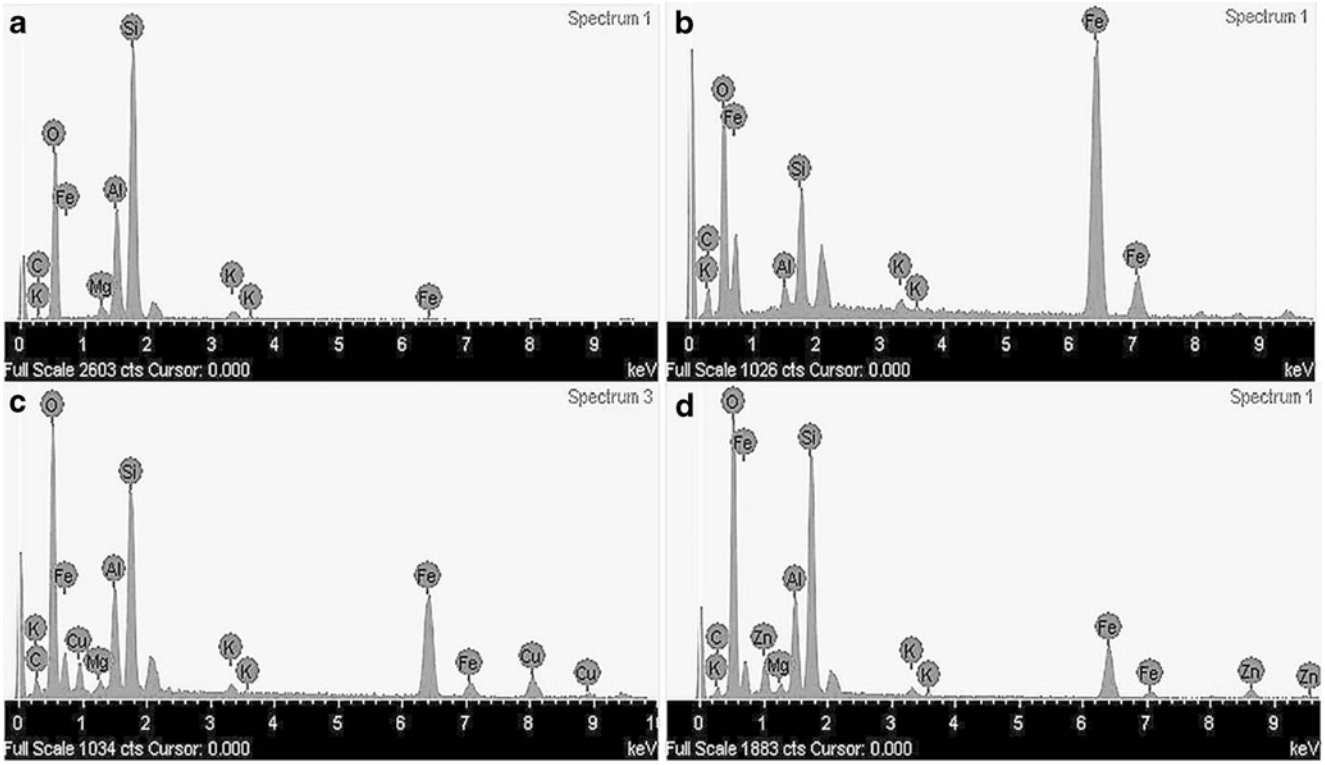

Fig. 4 EDX patterns of various solid samples. **a** Bentonite; **b** freshly synthesized B-nZVI (2:1); **c** B-nZVI (2:1) after reaction with Cu^{2+} solution; **d** B-nZVI (2:1) after reaction with Zn^{2+} solution

increase in the reactivity of nZVI after the dispersion of nZVI on the bentonite. In turn, this led to the stabilization of nZVI nanoparticles. This was also supported by previous studies on the reduction of nZVI aggregation and increase in reactivity using various support materials for nZVI nanoparticles (Ponder et al. 2000; Shahwan et al. 2010).

The EDS spectra of various materials are illustrated in Fig. 4. The EDS analysis of bentonite is shown in Fig. 4a, where the main composition of bentonite is 56.20 wt.% O, 27.59 wt.% Si and 9.15 wt.% Fe, while other all elements combined such as such as C, Mg, K and Fe are less than 5 %. Similar results obtained from EDS analysis of bentonite were observed (Vieira et al. 2010). However, Fig. 4b clearly demonstrates that Fe peaks are significantly increased in freshly synthesized B-nZVI (2:1) due to the dispersion of nZVI nanoparticles on bentonites, where the peaks of Fe are 48.31 and 20.82 wt.%, respectively. The increase in oxygen in freshly synthesized B-nZVI can be contributed to the oxidation of the nZVI surface in the atmosphere due to its core–shell structure (Li and Zhang 2007). As shown in Fig. 5c and d, the existence of Cu and Zn on the surface of B-nZVI after reaction was observed, confirming the adsorption of Cu^{2+} and Zn^{2+} onto the B-nZVI. The weight percentage of O in B-nZVI was 29.13 % before reacting and increased to 42.80 % and 52.28 %, respectively, after reacting with Cu^{2+} and Zn^{2+} solution. This could be ascribed to the oxidation process of the zero-valent iron in aqueous solution to form the FeOOH (Li and Zhang 2007).

Condition experiments and kinetics study

The pseudo-first-order model can be used to describe the reduction of Cu^{2+} and Zn^{2+} by nZVI as follows (Zhang et al. 2009):

$$\ln\frac{c}{c_0} = -k_{obs}t \tag{4}$$

where c (mg/l) and c_0 (mg/l) are the instantaneous concentration and initial concentration of contaminant, respectively, and k_{obs} (min^{-1}) is the observed rate constant.

Kinetics study of the simultaneous removal of Cu^{2+} and Zn^{2+} using B-nZVI under different conditions suggested that the removal of both ions was in accordance with the pseudo-first-order model with all correlation coefficients (R^2) higher than 0.99. The observed reaction rate constant can be obtained by calculating the slope of the linear regression slope as described in the following sections.

Effect of initial concentrations of Cu^{2+} and Zn^{2+}

By plotting $\ln(c/c_0)$ versus t, the kinetics of Cu^{2+} and Zn^{2+} removal using B-nZVI under initial concentrations are

presented in Fig. 5, which was described using the pseudo-first-order model. As shown in Fig. 5, for both ions the observed rate constant decreased as the initial concentrations increased. On the other hand, a lower rate of Zn^{2+} removal was obtained compared to Cu^{2+}, which was consistent with the previous section in the comparison study. For instance, k_{obs} decreased from 0.1620 to 0.0568 min^{-1} as the initial Cu^{2+} concentration increased from 20 to 100 mg/l, and the equilibrium time rose from 15 to 20 min, while the k_{obs} of Zn^{2+} removal fell from 0.1427 to 0.0111 min^{-1}. The equilibrium time rose from 20 to 40 min. Since the removal of both Cu^{2+} and Zn^{2+} was a surface-mediated process (Weber 1996; Li and Zhang 2007), this was attributed to the fact that the more the heavy metal ions approached the nZVI surface, the faster Fe^0 was oxidized into Fe(III). It formed a passivation layer on the surface of nZVI and subsequently resulted in the degeneration of reactivity (Yuan et al. 2009).

Effect of temperature

The k_{obs} of Cu^{2+} and Zn^{2+} removal under different temperatures was achieved by plotting ln c/c_0 versus time, which revealed that k_{obs} increased as temperature rose. A regression line can be achieved by plotting each k_{obs} versus reciprocal of corresponding temperature logarithmically with correlation coefficients (R^2) higher than 0.95. This allowed computation of E_a (Zhang et al. 2009):

$$\ln k_{obs} = -\frac{E_a}{RT} + \ln A_0 \quad (5)$$

where E_a (kJ/mol) is apparent activation energy, R (J/(mol K)) is the thermodynamic constant, T (K) is thermodynamic temperature, and A_0 represents the pre-exponential factor with the same dimension as k_{obs}.

The E_a of Cu^{2+} and Zn^{2+} using B-nZVI was 23.8 and 46.6 kJ/mol, respectively. The activation energy greater than 21.0 kJ/mol was proposed for chemically controlled adsorption processes (Geng et al. 2009). However, the low activation energy for Cu^{2+} suggests that the rate determining step of Cu^{2+} removal by B-nZVI was reduced rather than adsorption, while Zn^{2+} removal is the main adsorption. This was supported in the previous section when Cu^{2+} and Zn^{2+} were removed using various materials. Hence, it was concluded that surface reactions including adsorption and chemical reaction controlled the removal of Cu^{2+} and Zn^{2+} under experimental conditions.

On the basis of the results described above, the mechanism for removing Cu^{2+} and Zn^{2+} from aqueous solutions by using B-nZVI involves two strategies: one is that Cu^{2+} and Zn^{2+} in aqueous solution are adsorbed on the surface of B-nZVI since bentonite can absorb Cu^{2+} and Zn^{2+} (Mohan and Pittman 2006), and another is a scenario in which most of the adsorbed Cu^{2+} was reduced by Fe^0 or its corrosion products (Zhang 2003). However, Cu^{2+} removal by B-nZVI was reduced rather than adsorption, while Zn^{2+} removal was the main adsorption as Zn^{2+} has a more negative standard reduction of Zn^{2+}/Zn^0 than Fe^{2+}/Fe^0; it cannot be reduced by Fe^0 into Zn^0 in this reaction system, and it deposited on the B-nZVI in the form of Zn^{2+}. A possible mechanism is proposed below:

$$Fe^0 + 2H_2O \rightarrow Fe^{2+} + H_2 + 2OH^- \text{(in basic solution)} \quad (6)$$

$$\text{or } Fe^0 + 2H^+ \rightarrow Fe^{2+} + H_2 \text{(in acid solution)} \quad (7)$$

$$Cu^{2+}(Zn^{2+}) + \text{Bentonite} \rightarrow Cu^{2+}(Zn^{2+}) - \text{Bentonite(adsorption)} \quad (8)$$

$$Cu^{2+} - \text{Bentonite(adsorption)} + 2e \rightarrow Cu^0 - \text{Bentonite} \quad (9)$$

In addition, bentonite as a support material could stabilize and disperse nZVI as well as prevent nZVI from aggregation and thereby increase the reactivity of the nZVI despite the fact that B-nZVI has a lower surface area than nZVI; these also are confirmed by the evidence presented in this study.

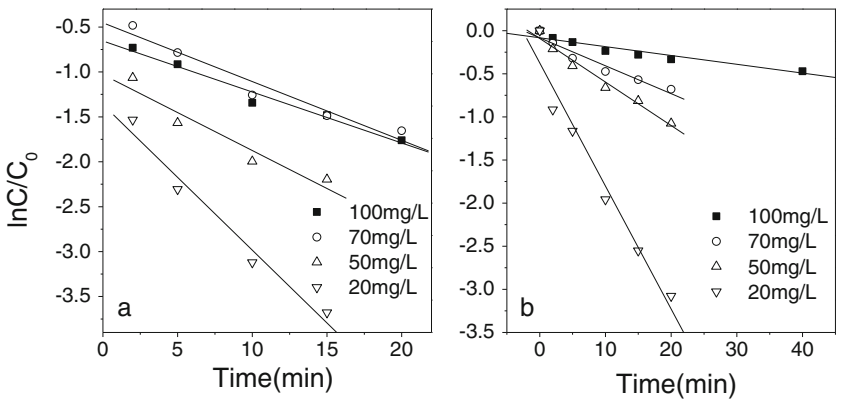

Fig. 5 The effects of the initial concentrations of Cu^{2+} and Zn^{2+} on their removal by B-nZVI (2:1). **a** Cu^{2+}; **b** Zn^{2+} (35 °C, C_0 (B-nZVI (2:1))=3 g/l, 250 rpm)

Table 1 Remediation of three different types of actual electroplating wastewater using B-nZVI

Waste water	Heavy metal	Total Cr	Pb^{2+}	Cu^{2+}	Zn^{2+}	Ni^{2+}
Electroplating wastewater I	C_0 (mg/l)	73±2	13.1±0.7	33.0±1.3	282±8	8.6[a]
	C' (mg/l)	[b]	[b]	11.1±0.3	195±7	[b]
	Remove amount (mg/g B-nZVI)	18.3	3.2	5.5	21.8	2.1
	Remove efficiency (%)	100	100	66.4	31.0	100
Electroplating wastewater II	C_0 (mg/l)	22.5±0.9	8.8±0.4	13.7±0.5	2.5[a]	14.7±0.5
	C' (mg/l)	[b]	[b]	[b]	[b]	[b]
	Remove amount (mg/g B-nZVI)	5.6	2.2	3.4	0.6	3.7
	Remove efficiency (%)	100	100	100	100	100
Dyeing wastewater	C_0 (mg/l)	12.5±0.4	2.4[a]	11.3±0.3	9.6[a]	[b]
	C' (mg/l)	[b]	[b]	[b]	[b]	[b]
	Remove amount (mg/g B-nZVI)	3.1	0.6	2.8	2.4	
	Remove efficiency (%)	100	100	100	100	100

The dosage of B-nZVI was 4 g/l

C_0 represents the initial concentrations of the heavy metals; C' represents the concentrations after reaction

[a] Standard deviations are too low to be presented

[b] The result is below the detection limit

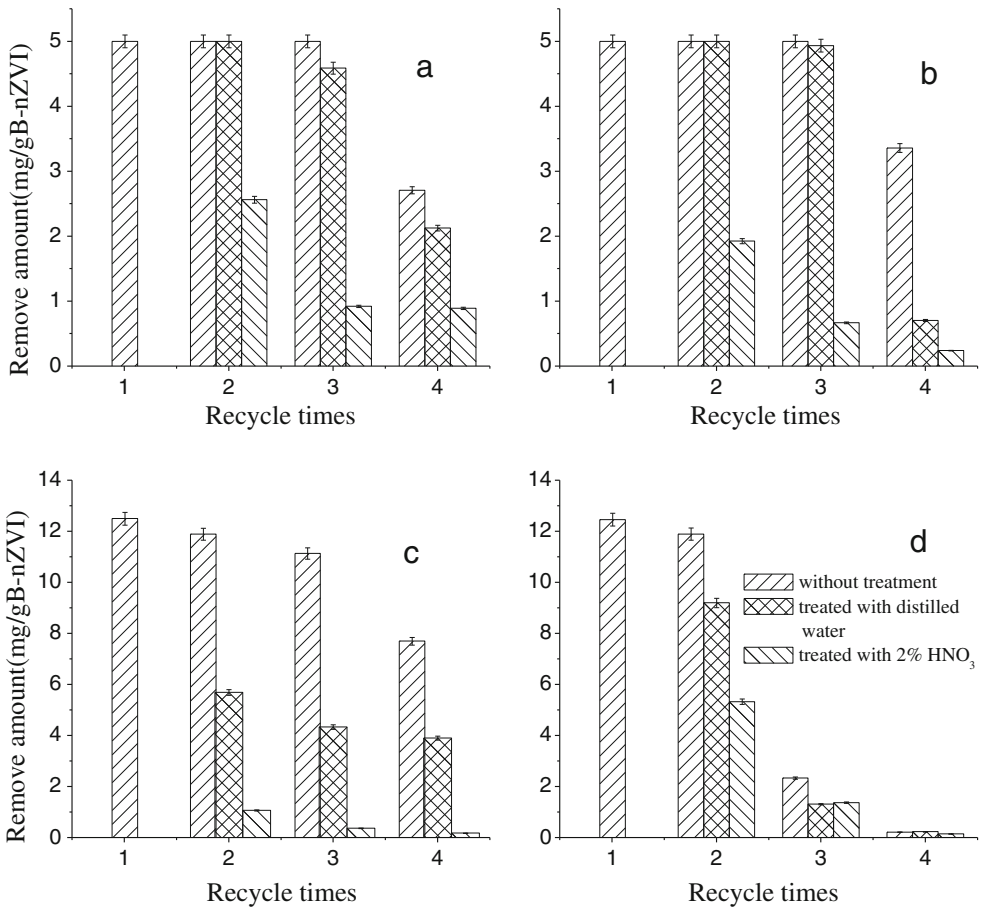

Fig. 6 Recycling of B-nZVI using different types of treatment. **a** Cu^{2+}, 20 mg/l; **b** Zn^{2+}, 20 mg/l; **c** Cu^{2+}, 50 mg/l; **d** Zn^{2+}, 50 mg/l

Removal of Cu^{2+} and Zn^{2+} from wastewaters by B-nZVI and B-nZVI reuse

Whether B-nZVI can be used to remove heavy metal ions and B-nZVI can be re-used to treat wastewaters containing heavy metal ions, were tested here. As listed in Table 1, the concentrations of total Cr, Pb^{2+}, Cu^{2+}, Zn^{2+} and Ni^{2+} ions in the wastewater were measured before and after reacting with B-nZVI. It can be seen that all heavy metals in wastewaters were undetected after reacting with 4 g/l of B-nZVI, except for Cu^{2+} and Zn^{2+} in electroplating wastewater I, which have high initial concentrations. Highly concentrated total Cr in electroplating wastewater I was completely removed because the reduction of Cr(VI) was favorable due to the much more positive standard reduction potential of Cr(VI)/Cr(III) ($\Phi^0_{Cr(VI)/Cr(III)}$=1.23 V) than Fe^{2+}/Fe^0. However, the initial pH values of three wastewaters were 2.0, 3.1 and 6.5, respectively, which increased to 4.7, 5.2 and 8.3 after reaction mainly because of the formation of OH^- when Fe^0 reacted with H_2O (Chen et al. 2008).

The reusability of B-nZVI in removing Cu^{2+} and Zn^{2+} is illustrated in Fig. 6 in terms of the amount removed by each unit mass of B-nZVI. Clearly, the heavy metals were completely removed with different initial concentrations when B-nZVI was first utilized. However, in the reuse cases, compared to the untreated B-nZVI, the removal of Cu^{2+} and Zn^{2+} decreased when B-nZVI treated either with distilled water or 2 % HNO_3 was undertaken. However, less amounts of Cu^{2+} and Zn^{2+} were removed when using treated B-nZVI with 2 % HNO_3. This could be ascribed to the excessive erosion by HNO_3 forming the iron oxide and reducing the reactivity of nZVI. The most durable reactivity was achieved using untreated B-nZVI with more than 50 % being removed even after three-time reuse, except for 50 mg/l Zn^{2+} solution. It indicated that a higher rate of removal of Cu^{2+} was obtained in all cases compared to Zn^{2+}. Furthermore, the reusability of B-nZVI was proven to be more effective when the initial heavy metal concentration was low, such as 20 mg/l. This can be explained by the limitation of its removal capacity, which was consistent with the reuse of kaolinite-supported nZVI to remove Cu^{2+} and Co^{2+} (Shahwan et al. 2010).

Conclusions

In this study, B-nZVI has been used to effectively remove Cu^{2+} and Zn^{2+} compared to nZVI supported by zeolite or kaolin. The reactivity of B-nZVI varied with the mass ratio of bentonite/nZVI, and the highest removal was achieved by B-nZVI (2:1). SEM images showed that the aggregation of nZVI decreased as the proportion of bentonite increased, which led to an increase in the SSA of nZVI. The removals of Cu^{2+} and Zn^{2+} by B-nZVI were consistent with the pseudo-first-order model kinetics, and k_{obs} rose as the initial concentrations of heavy metals decreased and temperature increased. B-nZVI can be used to remove various heavy metals from electroplating wastewaters. The reusability of B-nZVI was effective in removing Cu^{2+} and Zn^{2+} after being used four times. B-nZVI showed potential as a remediation agent that can be applied for in situ wastewater treatment.

Acknowledgements The project was supported by the Fujian "Minjiang Fellowship" from Fujian Normal University.

References

Bhattacharyya KG, Gupta SS (2008) Adsorption of a few heavy metals on natural and modified kaolinite and montmorillonite: a review. Adv Colloid Interface Sci 140:114–131

Chen S, Chen W, Shih C (2008) Heavy metal removal from wastewater using zero-valent iron nanoparticles. Water Sci Technol 58:1947–1954

Feng X, Wu Z, Chen X (2007) Removal of metal ions from electroplating effluent by EDI process and recycle of purified water. Sep Purif Technol 57:257–263

Geng B, Jin Z, Li T, Qi X (2009) Kinetics of hexavalent chromium removal from water by chitosan-Fe^0 nanoparticles. Chemosphere 75:825–830

Gupta VK, Nayak A (2011) Cadmium removal and recovery from aqueous solutions by novel adsorbents prepared from orange peel and Fe_2O_3 nanoparticles. Chem Eng J 180:81–90

Gupta VK, Rastogi A (2009) Biosorption of hexavalent chromium by raw and acid-treated green alga *Oedogonium hatei* from aqueous solutions. J Hazard Mater 163:396–402

Gupta VK, Sharma S (2003) Removal of zinc from aqueous solutions using bagasse fly ash−a low cost adsorbent. Ind Eng Chem Res 42:6619–6624

Gupta VK, Mittal A, Kurup L, Mittal J (2006) Adsorption of a hazardous dye, erythrosine, over hen feathers. J Colloid Interface Sci 304:52–57

Gupta VK, Jain R, Mittal A, Mathur M, Sikarwar S (2007a) Photochemical degradation of the hazardous dye Safranin-T using TiO_2 catalyst. J Colloid Interface Sci 309:464–469

Gupta VK, Jain R, Varshney S (2007b) Electrochemical removal of the hazardous dye Reactofix Red 3 BFN from industrial effluents. J Colloid Interface Sci 312:292–296

Gupta VK, Ali I, Saini VK (2007c) Defluoridation of wastewaters using waste carbon slurry. Water Res 41:3307–3316

Gupta VK, Mittal A, Malviya A, Mittal J (2009) Adsorption of carmoisine A from wastewater using waste materials—bottom ash and deoiled soya. J Colloid Interface Sci 335:24–33

Gupta VK, Rastogi A, Nayak A (2010) Adsorption studies on the removal of hexavalent chromium from aqueous solution using a low cost fertilizer industry waste material. J Colloid Interface Sci 342:135–141

Gupta VK, Agarwal S, Saleh TA (2011a) Chromium removal by combining the magnetic properties of iron oxide with adsorption properties of carbon nanotubes. Water Res 45:2207–2212

Gupta VK, Agarwal S, Saleh TA (2011b) Synthesis and characterization of alumina-coated carbon nanotubes and their application for lead removal. J Hazard Mater 185:17–23

Gupta VK, Ali I, T Saleh TA, Nayak A (2012a) Chemical treatment technologies for wastewater recycling: an overview. RSC Advances 2:6380–6388

Gupta VK, Pathania S, Agarwal S, Sharma S (2012b) Removal of Cr (VI) onto *Ficus carica* biosorbent from water. Environ Sci Pollut Res 19:1–13. doi:10.1007/s11356-012-1176-6

Gupta VK, Ali I, Saleh TA, Siddiqui M, Agarwal S (2012c) Chromium removal from water by activated carbon developed from waste rubber tires. Environ Sci Pollut Res 19:1–8. doi:10.1007/s11356-012-0950-9

Jain AK, Gupta VK, Jain S, Suhas (2004) Removal of chlorophenols using industrial wastes. Environ Sci Technol 38:1195–1200

Järup L (2003) Hazards of heavy metal contamination. Br Med Bull 68:167–182

Jiang MQ, Wang PQ, Jin XY, Chen ZL (2010) Removal of Pb(II) from aqueous solution using modified and unmodified kaolinite clay. J Hazard Mater 170:332–339

Keane M (1998) The removal of copper and nickel from aqueous solution using Y zeolite ion exchangers. Colloid Surf A Physicochem Eng Asp 138:11–20

Keith L, Telliard W (1979) ES&T special report: priority pollutants: a perspective view. Environ Sci Technol 13:416–423

Ladd MFC (2004) Introduction to physical chemistry, 3rd ed. Cambridge University Press, Cambridge

Li X, Zhang W (2006) Iron nanoparticles: the core shell structure and unique properties for Ni(II) sequestration. Langmuir 22:4638–4642

Li X, Zhang W (2007) Sequestration of metal cations with zerovalent iron nanoparticles. A study with high resolution X-ray photoelectron spectroscopy (HR-XPS). J Phys Chem C 111:6939–6946

Li X, Elliott DW, Zhang WX (2006) Zero-valent iron nanoparticles for abatement of environmental pollutants: materials and engineering aspects. Crit Rev Solid State Mater Sci 31:111–122

Lin X, Burns R, Lawrance G (2005) Heavy metals in wastewater: the effect of electrolyte composition on the precipitation of cadmium (II) using lime and magnesia. Water Air Soil Pollut 165:131–152

Mohan D, Pittman CU (2006) Activated carbons and low cost adsorbents for remediation of tri- and hexavalent chromium from water. J Hazard Mater 137:762–811

Nowack B, Bucheli TD (2007) Occurrence, behavior and effects of nanoparticles in the environment. Environ Pollut 150:5–22

Ponder SM, Darab JG, Mallouk TE (2000) Remediation of Cr (VI) and Pb (II) aqueous solutions using supported, nanoscale zero-valent iron. Environ Sci Technol 34:2564–2569

Saleh TA, Gupta VK (2011) Photo-catalyzed degradation of hazardous dye methyl orange by use of a composite catalyst consisting of multiwalled carbon nanotubes and titanium dioxide. J Colloid Interface Sci 371:101–106

Saleh TA, Gupta VK (2012) Column with CNT/magnesium oxide composite for lead (II) removal from water. Environ Sci Pollut Res 19:1224–1228

Sarioglu M, Güler UA, Beyazit N (2009) Removal of copper from aqueous solutions using biosolids. Desalination 239:167–174

Shahwan T, üzüm Eroglu A, Lieberwirth I (2010) Synthesis and characterization of bentonite/iron nanoparticles and their application as adsorbent of cobalt ions. Appl Clay Sci 47:257–262

Shi L, Lin Y, Zhang X, Chen Z (2011) Synthesis, characterization and kinetics of bentonite supported nZVI for the removal of Cr(VI) from aqueous solution. Chem Eng J 171:612–617

Vieira MGA, Almeida Neto AF, Gimenes ML, da Silva MGC (2010) Removal of nickel on bofe bentonite calcined clay in porous bed. J Hazard Mater 176:109–118

Wang QL, Lee SY, Choi HC (2010) Aging Study on the structure of Fe-nanoparticles: stabilization, characterization, and reactivity. J Phys Chem C 114:2027–2033

Weber E (1996) Iron-mediated reductive transformations: investigation of reaction mechanism. Environ Sci Technol 30:716–719

Yuan P, Fan M, Yang D, He H, Liu D, Yuan A, Zhu J, Chen T (2009) Montmorillonite-supported magnetite nanoparticles for the removal of hexavalent chromium [Cr(VI)] from aqueous solutions. J Hazard Mater 166:821–829

Zhang W (2003) Nanoscale iron particles for environmental remediation: An overview. J Nanopart Res 5:323–332

Zhang X, Lin YM, Chen ZL (2009) 2,4,6-Trinitrotoluene reduction kinetics in aqueous solution using nanoscale zero-valent iron. J Hazard Mater 165:923–927

Zhang X, Lin S, Chen ZL, Megharaj M, Naidu R (2011) Characterizations of kaolinite supported nanoscale zero-valent iron used to remove Pb^{2+} from aqueous solution. Water Res 45:3481–3488